NASA Technical Memorandum 107737

ON THE CROSS-STREAM SPECTRAL METHOD FOR THE ORR-SOMMERFELD EQUATION

William E. Zorumski
Steven L. Hodge

March 1993

National Aeronautics and Space Administration

Langley Research Center
Hampton, Virginia 23681-0001

Abstract

Cross stream modes are defined as solutions to the Orr-Sommerfeld equation which are propagating normal to the flow direction. These modes are utilized as a basis for a Hilbert space to approximate the spectrum of the Orr-Sommerfeld equation with plane Poiseuille flow. The cross-stream basis leads to a standard eigenvalue problem for the frequencies of Poiseuille flow instability waves. The coefficient matrix in the eigenvalue problem is shown to be the sum of a real matrix and a negative-imaginary diagonal matrix which represents the frequencies of the cross stream modes. The real coefficient matrix is shown to approach a Toeplitz matrix when the row and column indices are large. The Toeplitz matrix is diagonally dominant, and the diagonal elements vary inversely in magnitude with diagonal position. The Poiseuille flow eigenvalues are shown to lie within Geršgorin disks with radii bounded by the product of the average flow speed and the axial wavenumber. It is shown that the eigenvalues approach the Geršgorin disk centers when the mode index is large, so that the method may be used to compute spectra with an essentially unlimited number of elements. When the mode index is large, the real part of the eigenvalue is the product of the axial wavenumber and the average flow speed, and the imaginary part of the eigenvalue is identical to the corresponding cross stream mode frequency. The cross stream method is numerically well-conditioned in comparison to Chebyshev based methods, providing equivalent accuracy for small mode indices and superior accuracy for large indices.

1 Introduction

The Orr-Sommerfeld equation represents the small perturbations of otherwise parallel incompressible flow. As such, it has received a great deal of study. Most of these results are summarized in the excellent texts by Chandrasekhar [1] and by Drazin and Reid [2]. The primary objective of most investigations has been to define stability boundaries. These boundaries can be defined either by study of the growth and decay of modes in time or by study of their growth and decay in space. In either approach, it has been found advantageous to cast the problem in the form of a linear eigenvalue problem. Chandrasekhar [1], Dolph and Lewis [3], and Grosch and Salwen [4] used transcendental basis functions from fourth order operators to estimate eigenvalues of the Orr-Sommerfeld equation. Orzag [5] utilized Chebyshev polynomials in a study of the temporal eigenvalue problem, while Bridges and Morris [6] applied these polynomials in a study of the spatial formulation.

The movement toward Chebyshev polynomials was motivated by their attractive mathematical properties and by the disappointing results obtained from earlier approaches. Dolph and Lewis [3] had computed temporal eigenvalues using a set of basis functions derived from the Orr-Sommerfeld equation itself. Their rationale was that these functions would provide a natural basis for the problem at hand and could thus be expected to provide good approximations to the general Orr-Sommerfeld equation. The basis utilized by Dolph and Lewis was the countable set of solutions to the Orr-Sommerfeld equation for modes propagating perpendicular to the steady flow direction. For these modes, the Orr-Sommerfeld equation becomes a fourth-order ordinary differential equation with constant coefficients and thus has exact solutions given by the elementary transcendental functions.

But it is clear that Dolph and Lewis [3] were not entirely satisfied with their results. This may have been, in part, because they were still struggling with the numerics of the eigenvalue solution process, which is almost taken for granted today. The purpose of this paper is to re-examine the application of the basis functions of Dolph and Lewis [3] to the problem of determining the temporal stability characteristics of the Orr-Sommerfeld equation. Plane Poiseuille flow will be used for this study.

The characteristic solutions of the Orr-Sommerfeld equation are defined

by the system

$$\begin{aligned} L_4\phi &= \omega L_2\phi \\ \phi(\pm 1) &= 0 \\ \phi'(\pm 1) &= 0 \end{aligned}$$

where L_4 is a fourth order operator and L_2 is a second order operator. Let $\{\psi_0, \psi_1, \ldots\}$ be a *basis* for a Hilbert space with inner product $< u, v >$. A solution is defined by the expansion

$$\phi = \sum_{n=0}^{\infty} a_n \psi_n$$

which gives the matrix eigenvalue problem

$$\langle \psi_m, L_4\psi_n \rangle a_n = \omega \langle \psi_m, L_2\psi_n \rangle a_n$$

whose solutions give eigenvalues ω_i and associated eigenvectors a_{ni}. This paper compares two methods of solving the above eigenvalue problem for the case of Poiseuille flow. The first method utilizes the Chebyshev basis with the Lanczos tau criterion, and the second utilizes the cross-stream basis of Dolph and Lewis [3] with the Galerkin criterion.

Section 2 restates the Orr-Sommerfeld equation to define fully the operators and other notation. The Chebyshev/Tau method is applied to Poiseuille flow in section 3 and it is demonstrated that this method suffers from poor numerical conditioning. Section 4 develops the cross stream basis in detail and gives the procedures for evaluation the basis functions to machine precision. The cross stream formulation of the eigenvalue problem is given for general flows in section 5 and applied to the case of Poiseuille flow in section 6. The summary and conclusions are given in section 7.

2 The Orr-Sommerfeld Equation

The stability of incompressible flow in a channel is defined by characteristic solutions of the Orr-Sommerfeld equation. This paper presents an analysis of that equation emphasizing the special case of Poiseuile flow where the density and viscosity are constant. Figure 1 shows the flow in a channel. We use the same coordinates as in Drazin and Reid [2] since this is the most comprehensive and current work on the subject. In this system, x is the flow direction, y is horizontal and perpendicular to the flow, and z is vertical and perpendicular to the flow. The origin of coordinates is placed midway between the plates so that the lower and upper walls are located at $z = \pm h$.

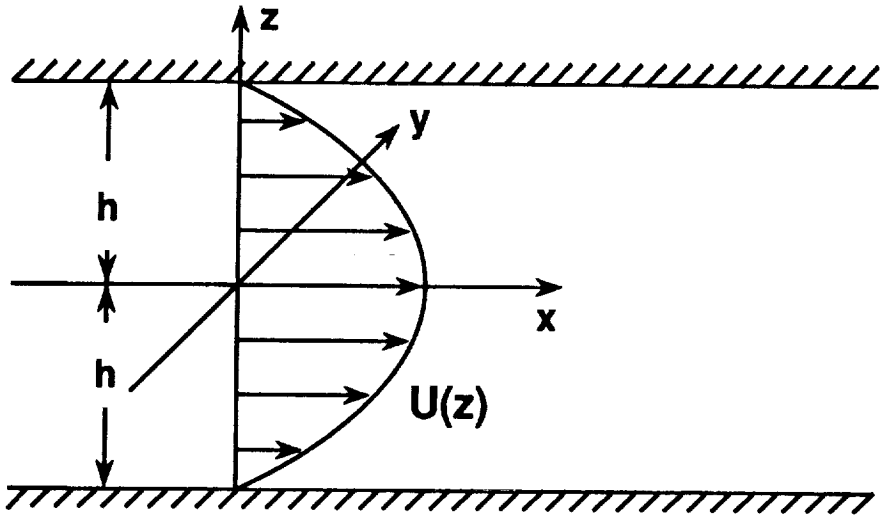

Figure 1: Poiseuille flow in a channel.

Poiseuille flow is formed by having an axial pressure gradient to induce the flow. The x-momentum equation for the steady flow gives

$$\frac{dp}{dx} = \frac{\partial \tau_{xz}}{\partial z} = \frac{\partial}{\partial z}\left(\mu \frac{\partial U}{\partial z}\right) = \text{ constant} \tag{1}$$

where μ is the viscosity. Since the shear stress gradient τ'_{xz} is constant, the stress varies linearly across the channel. The steady flow is then a parabola

and the maximum velocity is in the center of the channel.

$$U(z) = U_{max}\left(1 - \frac{z^2}{h^2}\right) \tag{2}$$

The Orr-Sommerfeld equation for velocity perturbations in the vertical direction (Drazin and Reid, [2, p. 156]) for a general velocity profile $U(z)$ is

$$(U_r - c_r)(w'' - k_r^2 w) + \frac{i\nu}{k_r}(w'''' - 2k_r^2 w'' + k_r^4 w) - U_r'' w = 0 \tag{3}$$

where $\nu = \mu/\rho$ is the kinematic viscosity.

The symbols in equation 3 are explained below in figure 2. The figure

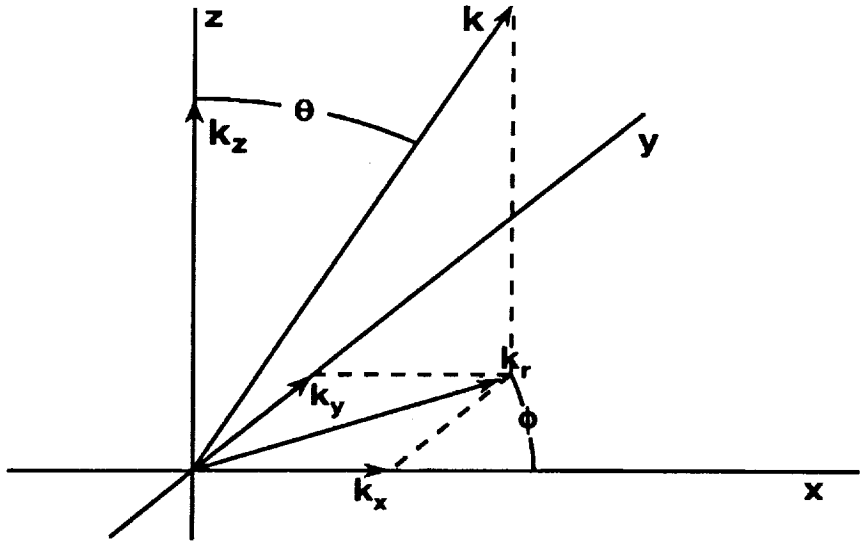

Figure 2: Coordinates and wavenumber conventions.

shows the wave vector geometry, which is taken according to a standard spherical coordinate convention.

$$\begin{aligned} \vec{k} &= k_x\vec{e}_x + k_y\vec{e}_y + k_z\vec{e}_z \\ k_r &= k\sin\theta \\ k_z &= k\cos\theta \\ k &= \sqrt{k_r^2 + k_z^2} \end{aligned} \tag{4}$$

$$
\begin{aligned}
k_x &= k_r \cos\phi \\
k_y &= k_r \sin\phi \\
k_r &= \sqrt{k_x^2 + k_y^2}
\end{aligned}
$$

Here k_r is the magnitude of the radial (horizontal) wave vector, which makes an angle ϕ with respect to the downstream flow velocity, that is

$$\phi = \arctan\left(\frac{k_y}{k_x}\right) \tag{5}$$

The polar angle θ is defined by the components k_r and k_z.

$$\theta = \arctan\frac{k_r}{k_z} \tag{6}$$

Here we have departed from Drazin and Reid is using k_x and k_y in place of their wavenumber symbols α and β. We also depart from their convention in showing the explicit dependence of the variables on the propagation angle ϕ. The component of $\vec{U}$ in the direction of the radial wave vector is $U_r = U\cos\phi$.

The vertical component of the perturbation velocity is assumed to be a wave of the form

$$we^{ik_r(\cos\phi\, x + \sin\phi\, y - c_r t)} \tag{7}$$

If we define a radial position vector

$$\vec{r} = \vec{e}_x x + \vec{e}_y y \tag{8}$$

then the fluctuating vertical velocity can be given in compact form

$$we^{i(\vec{k}_r\cdot\vec{r} - \omega t)} \tag{9}$$

Here, c_r is the complex radial propagation speed of the wave. The frequency of the wave is therefore

$$\omega = k_r c_r = k_r \cos\phi\, c = k_x c \tag{10}$$

where $c \equiv c_x$ is the complex downstream speed used by Drazin and Reid. We use nondimensional variables based on the maximum velocity U_{max}, and the channel half-width h. The non-dimensional frequency is then $\omega h/U_{max}$,

the non-dimensional wave number is $k_r h$, and the nondimensional kinematic viscosity is $\nu/(U_{max} h)$, which is the same as the inverse Reynolds number R^{-1}. The form of equation 3 remains the same, but we rewrite it as

$$i\nu L^4 w + k_r \cos\phi \left(U L^2 w - U'' w \right) = \omega L^2 w \tag{11}$$

where the operators are defined as follows

$$L^2 = \left(\frac{d^2}{dz^2} - k_r^2 \right) \tag{12}$$

$$L^4 = \left(\frac{d^4}{dz^4} - 2k_r^2 \frac{d^2}{dz^2} + k_r^4 \right) \tag{13}$$

For Poiseuille flow, the nondimensional flow velocity function and its second derivative would be

$$U = (1 - z^2) \tag{14}$$

$$U'' = -2 \tag{15}$$

3 Chebyshev/Tau Spectral Method

Orzag utilized a basis of Chebyshev polynomials with the Lanczos tau criterion to obtain accurate spectral solutions to the Orr-Sommerfeld equation for plane Poiseuille flow. This method is reviewed quickly here and Orzag's results are replicated as a basis for comparison to the cross-stream spectral method.

3.1 Review of the Chebyshev/Tau Method

The Chebyshev method utilizes a series representation of $w(z)$ in terms of the Chebyshev polynomials of the first kind.

$$w(z) = \sum_{n=0}^{\infty} a_n T_n(z) \tag{16}$$

It was shown by Orzag that the derivatives of $w(z)$ can be given by series of the same form as equation 16, provided that the coefficients in the series for the derivatives are defined in terms of the coefficients of the velocity function w. That is, the second derivative is given by the series

$$w''(z) = \sum_{n=0}^{\infty} a_n^{(2)} T_n(z) \tag{17}$$

where the coefficients in the series for the second derivative are defined in terms of the coefficients in the series for the function, i.e.

$$a_m^{(2)} = \frac{1}{c_m} \sum_{\substack{n=m+2 \\ n=m \,(\mathrm{mod}\ 2)}}^{\infty} n(n^2 - m^2) a_n, \quad m \geq 0 \tag{18}$$

where

$$c_m = \begin{cases} 0, & \text{if } m < 0; \\ 2, & \text{if } m = 0; \\ 1, & \text{if } m > 0. \end{cases} \tag{19}$$

Similar formulas for the fourth derivative are

$$w''''(z) = \sum_{n=0}^{\infty} a_n^{(4)} T_n(z) \tag{20}$$

$$a_m^{(4)} = \frac{1}{24c_m} \sum_{\substack{n=m+4 \\ n=m \,(\mathrm{mod}\ 2)}}^{\infty} P(m,n)a_n, \quad m \geq 0 \tag{21}$$

$$P(m,n) = n\left[n^2(n^2-4)^2 - 3m^2n^2(n^2-m^2) - m^2(m^2-4)^2\right] \tag{22}$$

These formulas are easily coded, but contain the origin of a significant problem of numerical conditioning. When placed in a matrix format by truncating the series to a finite number of terms, say a polynomial of degree $M+1$, the largest element in the matrix representing the fourth derivative operator is of order M^7. The derivative operator matrices are upper triangular, with zeros on the diagonal, and the matrix equivalent of the operator L^4 will have diagonal elements k_r^4, so that the smallest non-zero elements (on the diagonal) are of order unity, while the largest (in the upper right corner) are of order M^7.

In the case of Poiseuille flow, the only other relation needed is the expression for the function $z^2w(z)$. The formula for this term is found from known recurrence formulas for Chebyshev polynomials. As given by Orzag, the relation is

$$z^2w(z) = \frac{1}{4}\sum_{n=0}^{\infty}\left[c_{n-2}a_{n-2} + (c_n + c_{n-1})\,a_n + a_{n+2}\right] \tag{23}$$

The matrix equivalent of this series is a tri-diagonal matrix operator with simple fractional elements such $1/2$ and $1/4$. This matrix is designated here by the symbol $[Z^2]$.

Using the symbols $[L^2]$ and $[L^4]$ to designate the second and fourth order operators, respectively, the matrix equivalent of the Orr-Sommerfeld equation for Poiseuille flow is

$$k_x\left[2[I] + \left[[I] - [Z^2]\right][L^2]\right]\{a_n\} + i\nu[L^4]\{a_n\} = \omega[L^2]\{a_n\} \tag{24}$$

In the Lanczos tau method, the rows of the above matrix equation representing the highest-degree polynomials are replaced with the constraints representing the boundary conditions on w and w'. In this way, the boundary conditions are satisfied exactly by the solutions to the matrix eigenvalue problem.

Equation 24 has the form of a generalized eigenvalue problem, that is

$$Ax = \lambda Bx \tag{25}$$

Conversion of this equation to a standard eigenvalue problem would require a matrix inverse. While this is generally possible for matrices of reasonable size, the choice is usually to use direct methods, such as the QZ algorithm, for a direct solution of the generalized eigenvalue problem. The results presented below are from the IMSL [8] library routine GVCCG for the complex generalized eigenvalue problem. Measures of the accuracy of the computations were generated by the IMSL routine CPICG.

3.2 Results of the Chebyshev/Tau Method

Computations were made using the Chebyshev basis to find eigenvalues of the first 32 even modes, that is, where $n = \{0, 2, \cdots 62\}$. Results are shown in figure 3 for two computational word sizes, the 32-bit word and the 64-bit word. Points shown in the figure have been rotated through 90° in the complex plane by plotting $i\omega$ instead of ω. The first quadrant then contains eigenvalues of stable modes. The word size clearly has a strong effect

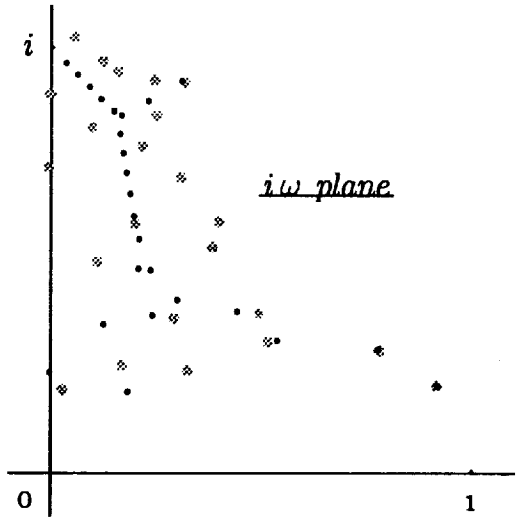

Figure 3: Computed eigenvalues $i\omega$ from the Chebyshev/Tau method. $k_r = 1.0$, $\phi = 0.0$, Re $= 10^4$, and 32nd order matrix. Gray symbols show results of 32-bit words, and black show results of 64-bit words.

on the results of the computation. The eigenvalues predicted by the 32-bit computation bear little or no relation to those predicted by the 64-bit computation, so that the less accurate computations must be incorrect. Accurate

computations with the Chebyshev basis require a large computer word. This is because the Chebyshev formulation is numerically ill-conditioned, that is, the condition numbers of the matrices in the generalized eigenvalue problem are large. The IMSL subroutine CPICG issued warnings that the 32-bit computations shown in figure 3 would be inaccurate.

There is another problem apparent in figure 3. One normally expects 32 eigenvalues from a 32nd order matrix, and a careful count of the points in figure 3 shows only 25 black symbols and 23 gray. Unless there are repetitions, the others must be off-scale, but where? The answer is that they are scattered hither and yon in the complex plane, far from the origin, and in all four quadrants. The black symbol just to the left of the imaginary axis, near the point $\Im[i\omega] = 2.2$, is normally called the"critical" eigenvalue, or fastest growing mode, but an examination of all the eigenvalues produced by this computation would indicate modes which grow much faster. Similar results are found also for the subcritical Reynolds numbers $\mathrm{Re} < 5772$. It would appear that researchers who report results of "critical eigenvalue" and "critical Reynolds number" computations from the Chebyshev/Tau method are exercising judgements about the spectra in their conclusions. While these opinions are no-doubt carefully considered and responsible, the need for such judgements presents a danger which becomes more significant when computations are made for problems which have been explored to a lesser extent. It is highly desirable to have a spectral method which is relatively insensitive to computer-word size and which produces spectra such that the least-attenuated mode can be defined absolutely by the maximum imaginary part of the eigenvalue. This paper will show that the cross-mode method achieves these computational goals.

4 Cross-Stream Modes

Dolph and Lewis [3] used solutions of the Orr-Sommerfeld equation with $\phi = \pm\pi/2$ as a *basis* for a spectral approximation. In this case, $\cos\phi = 0$, and the Orr-Sommerfeld reduces to

$$i\nu L^4 w = \omega L^2 w \tag{26}$$

The physical interpretation of these solutions is that the wave vector $\vec{k}_r$ is pointing across the flow direction, so that these solutions will be called cross-stream modes here.

4.1 Even Modes

An even solution is

$$w(z) = \frac{\alpha}{k}\left[\cos k_z z - \cos k_z \frac{\cosh k_r z}{\cosh k_r}\right] \tag{27}$$

where k is the spherical wavenumber and α is a constant to be defined later. This solution clearly satisfies the boundary conditions $w(\pm 1) = 0$. The boundary conditions $w'(\pm 1) = 0$ are then satisfied if

$$0 > k_z \tan k_z = -k_r \tanh k_r > -\infty, \quad 0 < k_r < \infty \tag{28}$$

The function $k_z \tan k_z$ in equation 28 is even and, when k_z is small, approaches k_z^2. Since $k_r \tanh k_r$ is even also, it approaches k_r^2 when k_r is small. But there is no "small-k_z" solution to equation 28 because $k_z \tan k_z$ is positive while $-k_r \tanh k_r$ is negative. The first solution $k_{z0} > 0$ is thus found in the interval $(\pi/2 < k_{z0} < \pi)$. Since $k_z \tan k_z$ is monotonically increasing in this interval, there is one and only one solution within the interval. Since the solutions k_{zn} to equation 28 are real positive numbers, the following change of variable is introduced to facilitate their computation.

$$k_{zn}(k_r) = \kappa_n - \delta_n(k_r) \tag{29}$$

$$\kappa_n = \left(\frac{n+2}{2}\right)\pi \tag{30}$$

Then equation 28 becomes

$$\tan \delta_n = \frac{\beta_n}{\kappa_n - \delta_n}, \quad \beta_n(k_r) = k_r \tanh k_r, \quad n = 0, 2, 4, \cdots \tag{31}$$

This equation has a unique solution $0 \leq \delta_n(k_r) < \pi/2$ for each selected even index n. Thus, equation 28 has a countable set of solutions which may be labled by the set of non-negative even integers. When k_r is large, δ_n approaches $\pi/2$, and the solutions k_{zn} approach $(n+1)\pi/2$ from above. When k_r is small, $\delta_n(k_r)$ approaches 0, and the solutions k_{zn} approach $(n+2)\pi/2$ from below.

Asymptotic formulas for the solutions $\delta_n(k_r)$ of equation 31 can be found by writing it as an arctangent function of the parameter κ_n.

$$\delta(\epsilon_n) = \arctan\left[\frac{\beta_n \epsilon_n}{1 - \epsilon_n \delta(\epsilon_n)}\right], \quad \epsilon_n = \kappa_n^{-1} \tag{32}$$

A Taylor series in the parameter ϵ_n then gives the desired formula.

$$\delta_n \sim \frac{\beta_n}{\kappa_n} + \frac{(3 - \beta_n)\beta_n^2}{3\kappa_n^3} + \frac{(30 - 20\beta_n + 3\beta_n^2)\beta_n^3}{15\kappa_n^5} + \cdots, \quad n \to \infty \tag{33}$$

Although it is valid in concept only for large n, when $\kappa_n >> k_r$, this formula is valid to four digits even in the case $n = 0$, $k_r = 1.0$, $\kappa_0 = \pi$. It thus provides a good initial estimate for a numerical solution of equation 32 for moderate values of k_r.

Numerical solutions for the wavenumbers are based on equation 32, written as a function of a variable $0 \leq \xi = 2\delta_n/\pi < 1$ together with its first derivative.

$$f_n(\xi) = \xi - \frac{2}{\pi} \arctan\left[\frac{\gamma_n}{(n+2) - \xi}\right] \tag{34}$$

$$f_n'(\xi) = 1 - \frac{2}{\pi} \frac{\gamma_n}{[(n+2) - \xi]^2 + \gamma_n^2} \tag{35}$$

where

$$\gamma_n = \frac{2\beta_n}{\pi} \tag{36}$$

Figure 4 shows these functions for $n = 0, 1, 2, \infty$. The functions are nearly straight lines, so that the zero-crossing points $\xi_0(n)$ are easily found numerically. The slopes of the curves are positive and nearly unity, so that the

errors in the functions are roughly the same as the error in the solution. The solutions are found by starting with the estimate of the asymptotic formula 33 and then iterating with Newtons method using equations 34, 35 until a desired accuracy is reached. Using a 64-bit computer word, which is equivalent to about 15 digits accuracy, the numerical solutions have been computed with an error no greater than 10^{-14}.

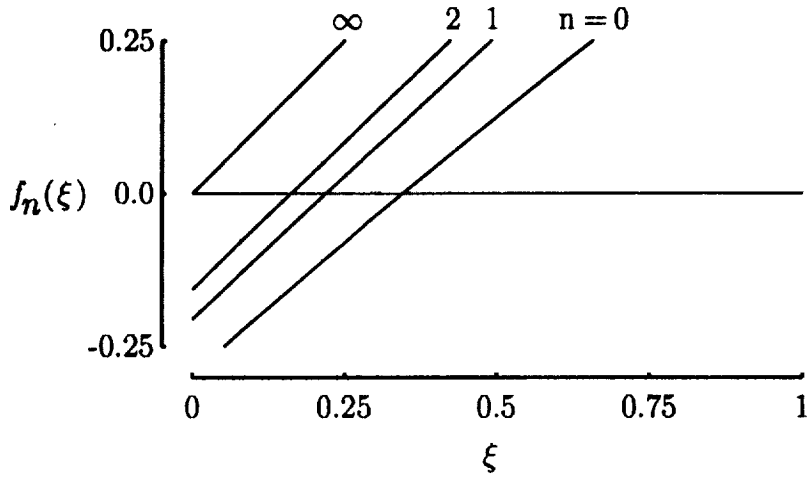

Figure 4: Graphical solution for vertical wavenumbers, $\gamma_n = 1$.

4.2 Odd Modes

An odd solution to equation 26 is

$$w(z) = \frac{\alpha}{k}\left[\sin k_z z - \sin k_z \frac{\sinh k_r z}{\sinh k_r}\right] \tag{37}$$

The characteristic equation is again given by the boundary conditions on w'

$$1 > \frac{1}{k_z}\tan k_z = \frac{1}{k_r}\tanh k_r > 0, \quad 0 < k_r < \infty \tag{38}$$

Equation 38 also has a countable set of solutions. Since $(\tan k_z)/(k_z) \geq 1$ in the interval $(-\pi/2, \pi/2)$ and since $(\tanh k_r)/k_r < 1$ in the interval $0 < k_r < \infty$, there is no solution within the central interval $(-\pi/2 < k_z < \pi/2)$.

However, there is a single solution within each interval $((n+1)\pi/2 < k_{zn} < (n+2)\pi/2,\ n = 1,3,5\cdots$.Therefore, equation 38 has a countable set of solutions which may be labeled by the positive odd integers. When k_r is large, these solutions approach $(n+1)\pi/2$ from above (but now n is odd), and, when k_r is small, they approach a limit from below, but the limit is less than $(n+2)\pi/2$. Using the same offset variable definition as in the case of even modes, but with odd indices n, equation 38 is written in arctangent form.

$$\delta(\epsilon_n) = \arctan\left[\frac{\beta_n \epsilon_n}{1 - \epsilon_n \delta(\epsilon_n)}\right], \quad \beta_n(k_r) = k_r \coth k_r, \quad n = 1,3,5,\cdots \quad (39)$$

This equation is identical to the one for the even mode wavenumbers, except for the definition of β_n, so that the asymptotic formula 33 and the function for numerical solution, equation 34 are applicable to the odd modes as well as the even.

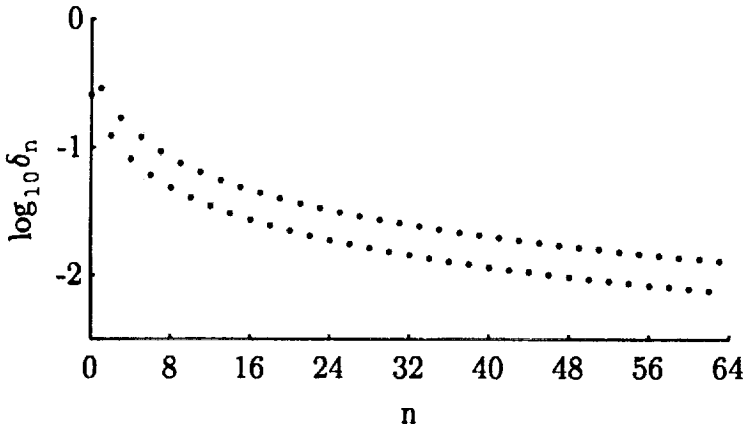

Figure 5: Wavenumber offsets for 64 modes, $k_r = 1$.

Figure 5 shows the wavenumber offsets δ_n as computed by the asymptotic formula. The points are plotted as $\log_{10}\delta_n$ versus n. There are two patterns— the "upper" points are the odd indices, and the "lower" are the even. This is because the function $\beta_n(k_r)$ is always larger for the odd indices. These offset variables become small quickly as the mode index increases. Consequently, the small-angle approximations for $\sin\delta_n$ and $\cos\delta_n$ will be

accurate for all but possibly the "lowest" modes. Figure 6 shows the accuracy of the asymptotic formula for the offsets, compared to the numerical solution of the offset equation by Newton's method. The asymptotic formula

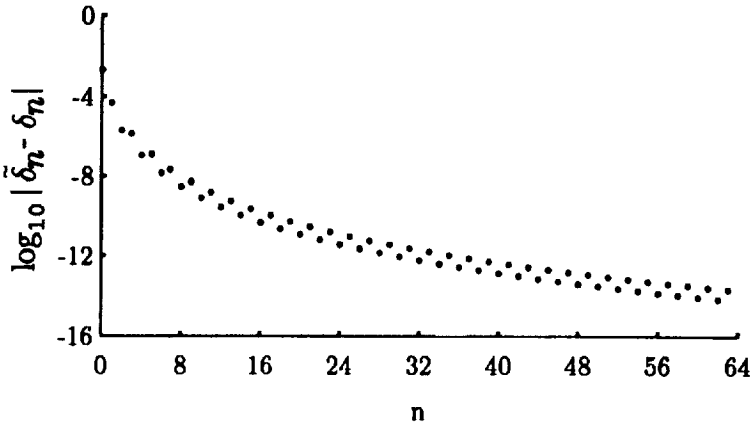

Figure 6: Accuracy of asymptotic formula for wavenumber offsets for 64 modes, $k_r = 1$.

has an absolute error less than 10^{-12} for mode indices greater than about 48. The formula is more accurate for the even indices than for the odd, but is an excellent approximation in either case.

4.3 Combined Modes

4.3.1 Definitions and identities

The combined set of all real-valued solutions to equation 28 and to equation 38 is thus a countable set of distinct wavenumbers which increase monotonically with the index n.

$$\{\frac{\pi}{2} < k_{z0} \leq \pi < k_{z1} < \frac{3\pi}{2} < k_{z2} \leq 2\pi < \cdots\} \tag{40}$$

Associated with these wavenumbers are characteristic solutions, called cross-modes here. It will be helpful to utilize the following identities in the definition of these modes.

$$\cos k_{zm} = -(-1)^{[m/2]} \cos \delta_m, \quad m \text{ even} \tag{41}$$

$$\sin k_{zm} = -(-1)^{[m/2]} \cos \delta_m, \quad m \text{ odd} \tag{42}$$

The cross-modes are then defined as linear combinations of two "mode parts" $\phi_n(z)$ and $\psi_n(z)$.

$$w_n(z) = \frac{\alpha_n}{k_n}\left[\phi_n(z) + (-1)^{[n/2]} \cos \delta_n \psi_n(z)\right] \quad n = 0, 1, 2 \cdots \tag{43}$$

$$\phi_n(z) = \begin{cases} \cos k_{zn} z, & n \text{ even} \\ \sin k_{zn} z, & n \text{ odd} \end{cases} \tag{44}$$

$$\psi_n(z) = \begin{cases} \cos ik_r z / \cos ik_r, & n \text{ even} \\ \sin ik_r z / \sin ik_r, & n \text{ odd.} \end{cases} \tag{45}$$

The function $\psi_n(z)$ is usually expressed in terms of real hyperbolic functions, but it will be convenient later to use the complex forms shown in equations 45. Note that the division operation $[n/2]$ in equation 43 is an integer operation with an integer result.

It is easy to show that

$$L^2 \psi_n(z) = 0 \tag{46}$$

$$L^2 \phi_n(z) = -k_n^2 \phi_n(z) \tag{47}$$

$$L^2 w_n(z) = -\alpha_n k_n \phi_n(z) \tag{48}$$

These results will be useful later in the development of spectral approximations to Orr-Sommerfeld equation.

4.3.2 Inner products, norms, and orthogonality

An inner product is defined as an integral over the interval [-1,1].

$$\langle f, g \rangle = \frac{1}{2} \int_{-1}^{1} f(z) g(z)\, dz \tag{49}$$

The natural norm of a function is the square root of the inner product of the function with itself.

$$||f|| = \langle f, f \rangle^{1/2} \tag{50}$$

The constants α_n can be defined using the above definitions and the orthonormal condition of Dolph and Lewis [3]

$$\frac{1}{2} \int_{-1}^{1} \left[k_r^2 w_m(z) w_n(z) + w_m'(z) w_n'(z)\right] dz = \delta_{mn} \tag{51}$$

Integrating equation 51 by parts and using the definition 49 gives the identity

$$\langle w_m, -L^2 w_n \rangle = \delta_{mn} \tag{52}$$

The cross-stream modes $w_n(z)$ are not orthogonal; however, they are "partly orthogonal", meaning that their two parts, as given by equation 41, are orthogonal. More precisely, the orthogonality properties of the two parts are

$$\langle \phi_m, \psi_n \rangle = 0, \quad \text{all } m, n \tag{53}$$

Since the functions ψ are either even or odd, depending on the parity of the index, there is also the condition

$$\langle \psi_m, \psi_n \rangle = 0, \quad m+n \text{ odd} \tag{54}$$

It can also be shown, using the characteristic equations for k_{zn}, that the functions ϕ_n are orthogonal.

$$\langle \phi_m, \phi_n \rangle = \delta_{mn} \langle \phi_n, \phi_n \rangle \tag{55}$$

Combining this result with equation 52 defines the constants α_n through the following equation.

$$\alpha_n = \langle \phi_n, \phi_n \rangle^{-1/2} = ||\phi_n||^{-1} \tag{56}$$

The inner product $\langle \phi_n, \phi_n \rangle$ is given by

$$\langle \phi_n, \phi_n \rangle = \frac{1}{2} \left(1 + (-1)^n \operatorname{sinc} 2k_{zn}\right) \tag{57}$$

where the "sinc" function is defined as

$$\operatorname{sinc} x = \frac{\sin x}{x} \tag{58}$$

Similarly, the inner product of the function ψ_n with itself is

$$\langle \psi_n, \psi_n \rangle = \frac{1 + (-1)^n \operatorname{sinch} 2k_r}{1 + (-1)^n \cosh 2k_r} \tag{59}$$

with

$$\operatorname{sinch} x = \frac{\sinh x}{x} \tag{60}$$

Using the expression for the vertical wavenumbers gives

$$\langle \phi_n, \phi_n \rangle = \frac{1}{2}\left(1 - \frac{\sin 2\delta_n}{2k_{zn}}\right) \tag{61}$$

and the norm of the function ϕ_n is

$$||\phi_n|| = \frac{\sqrt{2}}{2}\left(1 - \frac{\sin 2\delta_n}{2k_{zn}}\right)^{1/2} \tag{62}$$

Since $\delta_n \to 0$ for large n, it is clear that the above inner product approaches $1/2$. The final formula for the constants is then

$$\alpha_n = \sqrt{2}\left(1 - \frac{\sin 2\delta_n}{2k_{zn}}\right)^{-1/2} \tag{63}$$

Note that $\alpha_n = O(\sqrt{2})$ for all values of k_r and n. The norm $||\phi_n||$ is a positive real number, roughly $\sqrt{2}/2$ for any k_r, including the limits where $k_r \to 0$ and $k_r \to \infty$. The norm of the function ψ_n is

$$||\psi_n|| = \frac{1}{\sqrt{2k_r}}\left(\frac{\sinh 2k_r \pm 2k_r}{\cosh 2k_r \pm 1}\right)^{1/2}, \quad \begin{cases} + & \text{if } n \text{ is even,} \\ - & \text{if } n \text{ is odd.} \end{cases} \tag{64}$$

The norm $||\psi_n||$ approaches a positive limit, 1 for even modes and $\sqrt{3}/3$ for odd, as k_r approaches zero and approaches zero in the limit of large k_r. The cross-mode functions are defined finally using the norm of the functions ϕ_n.

$$w_n = \frac{\phi_n + (-1)^{[n/2]} \cos\delta_n \psi_n}{k_n ||\phi_n||} \tag{65}$$

The norm of the cross-mode w_n is

$$||w_n|| = \frac{\left(||\phi_n||^2 + \cos^2\delta_n ||\psi_n||^2\right)^{1/2}}{k_n ||\phi_n||} \tag{66}$$

These results show that the cross-modes, as defined here, approach 0 uniformly in z when either k_r or n becomes large, because the magnitude of the spherical wavenumber k_n becomes large. The derivatives of the cross-modes are finite, however, for these cases. The Dolph-Lewis normalization

condition, equation 51 can be given in terms of the norms $||w_n||$ and $||w_n'||$ as

$$||w_n'||^2 + k_r^2||w_n||^2 = 1 \tag{67}$$

This is the equation for an ellipse with $||w_n||$ plotted as the abscissa and $||w_n'||$ plotted as the ordinate. The "semi-major" axis is k_r^{-1}. , and the "semi-minor" axis is 1. Of course, if $k_r > 1$ the major axis becomes the ordinate instead of the abscissa. But this equation makes clear the following bounds on the norms of w_n and w_n'.

$$||w_n|| < k_r^{-1} \tag{68}$$
$$||w_n'|| < 1 \tag{69}$$

There is also the following explicit equation for the norm of the derivative in terms of the norms of the mode parts.

$$||w_n'||^2 = \frac{k_{zn}^2||\phi_n||^2 - k_r^2\cos^2\delta_n||\psi_n||^2}{k_n^2||\phi_n||^2} \tag{70}$$

The ratio k_{zn}/k_n approaches unity for large k_{zn}, consequently, for fixed k_r and large index n, the norms have the following asymptotic limits.

$$||w_n|| \sim 0, \quad n \to \infty \tag{71}$$
$$||w_n'|| \sim 1, \quad n \to \infty \tag{72}$$

Figures 7 and 8 illustrate the cross-modes and the norm properties described above. Figure 7 is the lowest mode, $n = 0$. Only the domain $[0 \leq z \leq 1]$ is shown because the mode is even. The solid curve is the mode function $w_n(z)$ and the dashed curve is its derivative $w_n'(z)$. Note that both curves approach zero at the boundary as required by the boundary conditions. The norms of the function and its derivative are similar in magnitude for this mode.

Figure 8 shows the eighth cross-mode. It is clear that the mode has smaller norm than its derivative norm in this case. The derivative of the mode is roughly a sine function. The norm of the derivative, which is the rms value taken over the channel width, is near unity for this mode.

The cross-modes are non-orthogonal, or non-normal. A measure of relative normality of different modes is the "angle" γ_{mn} between two different

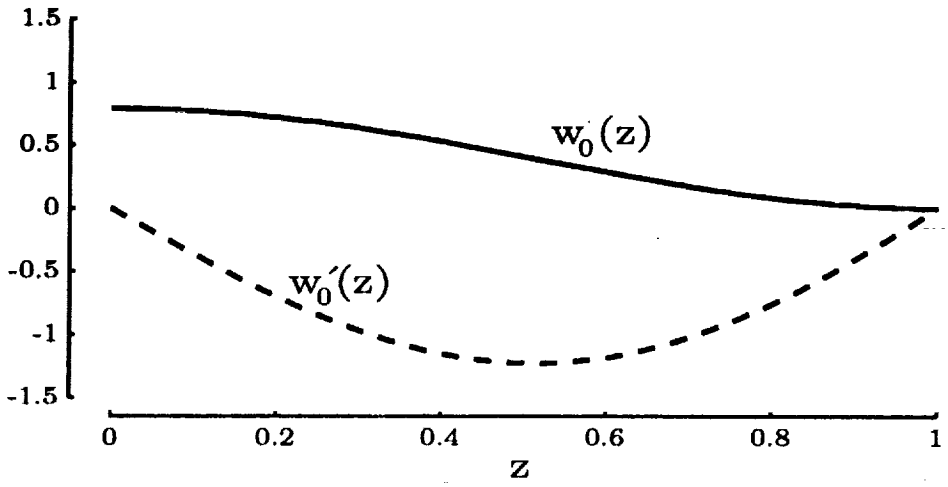

Figure 7: Cross mode $w_0(z)$ and its derivative $w_0'(z)$, $k_r = 1$.

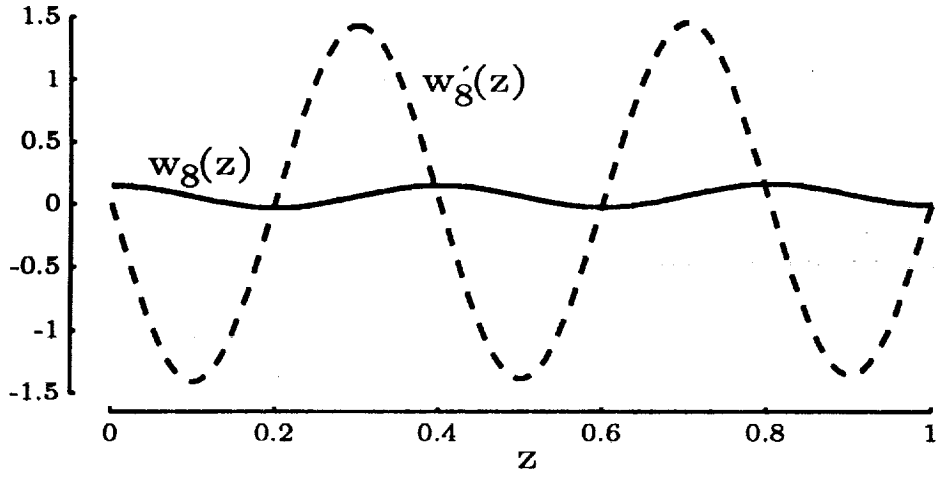

Figure 8: Cross mode $w_8(z)$ and its derivative $w_8'(z)$, $k_r = 1$.

modes. This angle can be defined as

$$\cos\gamma_{mn} = \frac{\langle w_m, w_n\rangle}{||w_m|| \cdot ||w_n||} \tag{73}$$

The angle between any mode and itself is zero, because this formula gives $\cos\gamma_{mm} = 1$. The angle between modes of opposite parity is $\pi/2$, because the inner product $\langle w + m, w_n\rangle$ is zero. The remaining case to consider is the angle between two modes of the same parity, where $m+n$ is an even number. In this case, the angle is

$$\cos\gamma_{mn} = \frac{(-1)^{[m/2]+[n/2]}\cos\delta_m\cos\delta_n\,||\psi_m||\cdot||\psi_n||}{\left(||\phi_m||^2 + \cos^2\delta_m\,||\psi_m||^2\right)^{1/2}\left(||\phi_n||^2 + \cos^2\delta_n\,||\psi_n||^2\right)^{1/2}} \tag{74}$$

The sine of the angle γ_{mn} is conveniently defined by a two-equation formula as follows.

$$a_m = \cos\delta_m\frac{||\psi_m||}{||\phi_m||} \tag{75}$$

$$\sin\gamma_{mn} = \left(\frac{1 + a_m^2 + a_n^2}{1 + a_m^2 + a_n^2 + a_m^2 a_n^2}\right)^{1/2} \tag{76}$$

In a typical case, the norms are of the same order of magnitude, and $\sin\gamma_{mn} \approx \sqrt{3}/2$. The angle between the modes would be roughly 60°. In the case where $k_r = 1$, the angles between all even modes is about 57°, and the angles between all odd modes is about 68°.

The frequencies ω_n associated with the cross-stream modes are

$$\omega_n = -i\nu(k_r^2 + k_{zn}^2) = -i\nu k_n^2 \tag{77}$$

Note that the frequencies are inversely proportional to the Reynolds number and are separated by roughly $-i\nu(2n+3)\pi^2/4$. When the Reynolds number is large, there will be a considerable number of frequencies on the negative imaginary axis whose magnitude is small, but these frequencies are always distinct, that is, they form a discrete set. Waves corresponding to these frequencies decay slowly in time, but are absolutely stable. Note that, since $k_{z0} > \pi/2$, the "closest" frequency ω_0 is "below" $-i\nu(k_r^2 + \pi^2/4)$ on the imaginary axis.

5 Cross-Stream Spectral Method

5.1 Standard Eigenvalue Equation

The solutions of the cross stream propagation case may be useful in a spectral approximation for the general case. Since each solution satisfies the boundary conditions, a representation of $w(z)$ by an infinite sum of these terms will also satisfy the boundary conditions. We therefore seek an spectral solution to the Orr-Sommerfeld equation by using the Galerkin criterion. Thus, let

$$w(z) = \sum_{n=0}^{\infty} a_n w_n(z)/k_n = \lfloor\, w_n(z)/k_n \,\rfloor \{\, a_n \,\} \tag{78}$$

where it is clear that the row matrix has dimensions $(1, \infty)$ and the column has dimensions $(\infty, 1)$. If the sequence a_n is bounded for large n, then the series converges as k_n^{-2} because the norm of w_n is proportional to k_n^{-1}. This spectral solution in the Orr-Sommerfeld equation gives an equation

$$i\nu \lfloor\, L^4 w_n/k_n \,\rfloor \{\, a_n \,\} + k_x \lfloor\, (UL^2 - U'')w_n/k_n \,\rfloor \{\, a_n \,\} = \omega \lfloor\, L^2 w_n/k_n \,\rfloor \{\, a_n \,\} \tag{79}$$

This equation can be simplified somewhat by using the equation for the cross stream modes, a special case of equation 79 which is satisfied identically for each term in the series.

$$i\nu \lfloor\, L^4 w_n/k_n \,\rfloor \{\, a_n \,\} = \lfloor\, \omega_n L^2 w_n/k_n \,\rfloor \{\, a_n \,\} \tag{80}$$

Subtracting equation 80 from equation 79 gives the simplified approximation

$$k_x \lfloor\, (UL^2 - U'')w_n/k_n \,\rfloor \{\, a_n \,\} = \lfloor\, (\omega - \omega_n) L^2 w_n/k_n \,\rfloor \{\, a_n \,\} \tag{81}$$

Any error in this solution must be orthogonal to the elements $w_m(z)$ of the set of cross-stream basis functions. This gives the linear eigenvalue problem

$$k_x \left[\, k_m \langle w_m, (-UL^2 + U'')w_n/k_n \rangle \,\right] \{\, a_n \,\} + [\,\omega_n\,] \{\, a_n \,\} = \omega \{\, a_n \,\} \tag{82}$$

Equation 82 can be stated concisely as

$$[k_x[D] + [\omega_n]] \{\, a_n \,\} = \omega \{\, a_n \,\} \tag{83}$$

where it is understood that $[\omega_n]$ is a diagonal matrix and the matrix $[D]$ is given by

$$[D] = [\, k_m \langle w_m, (-UL^2 + U'')w_n \rangle / k_n \,] \tag{84}$$

The above equations are given in terms of infinite matrices, and the computations must be restricted to finite matrices. It is assumed here, and will be demonstrated later, that a convergence occurs as the matrix size increases. But no proof of convergence will be attemped. Further discussion of the convergence of spectral approximations may be found in the book by F. Chatelin [7].

The matrix $[D]$ is a function of k_r only. Once this is constructed, the dependence of the eigenvalues on $\cos\phi$ can be observed by repeated solutions with different values of that parameter. The matrix $[D]$ is real, but not symmetric. It is clear that the eigenvalues of equation 83, viewed as a function of ϕ, will be stationary at the downstream direction $\phi = 0$. This is consistent with Squire's theorem, which says that the imaginary parts of the eigenvalues take on extremal values at that point. The effect of Reynolds number is contained within the cross-mode frequencies ω_n. These frequencies are negative imaginary numbers which are inversely proportional to Reynolds number and directly proportional to the square of the spherical wave number.

5.2 Evaluation of the array D_{mn}

The elements of the matrix will be designated by D_{mn}, with m indicating the row number and n indicating the column. Using the identity 46 gives

$$D_{mn} = k_m \langle U, w_m \phi_n \rangle \alpha_n + k_m \langle U'', w_m w_n \rangle / k_n \tag{85}$$

The classic cases of Couette and Poiseuille flow are included within the case where $U(z)$ is a polynomial of degree $p \geq 2$.

$$U(z) = \sum_{j=0}^{p} u_j z^j \tag{86}$$

$$U''(z) = \sum_{j=0}^{p-2} u''_j z^j \tag{87}$$

$$u''_j = (j+2)(j+1)u_{j+2} \tag{88}$$

Equation 85 is rewritten for the polynomial velocity profile with inner products of powers of z and products of the mode functions.

$$D_{mn} = \sum_{j=0}^{p} u_j k_m \langle z^j, w_m \phi_n \rangle \alpha_n + \sum_{j=0}^{p-2} u_j'' k_m \langle z^j, w_m w_n \rangle / k_n \tag{89}$$

This rewritten form shows that it is necessary only to evaluate three different arrays. These are

$$A_{jmn} = \langle z^j, \phi_m \phi_n \rangle \tag{90}$$
$$B_{jmn} = \langle z^j, \psi_m \phi_n \rangle \tag{91}$$
$$C_{jmn} = \langle z^j, \psi_m \psi_n \rangle \tag{92}$$

The other array is a transpose of the second one above

$$\langle z^j, \phi_m \psi_n \rangle = B_{jnm} = B_{jmn}^T \tag{93}$$

Now, the array D_{mn} is given by the long expression

$$\begin{aligned} D_{mn} &= \alpha_m \alpha_n \sum_{j=0}^{p} u_j \left(A_{jmn} + (-1)^{[m/2]} \cos \delta_m B_{jmn} \right) \\ &+ \frac{\alpha_m \alpha_n}{k_n^2} \sum_{j=0}^{p-2} u_j'' \left(A_{jmn} + (-1)^{[m/2]+[n/2]} \cos \delta_m \cos \delta_n C_{jmn} \right) \\ &+ \frac{\alpha_m \alpha_n}{k_n^2} \sum_{j=0}^{p-2} u_j'' \left((-1)^{[m/2]} \cos \delta_m B_{jmn} + (-1)^{[n/2]} \cos \delta_n B_{jmn}^T \right) \end{aligned} \tag{94}$$

5.2.1 Evaluation of arrays A_{jmn}

The elements of the array A_{jmn} are given by the formula

$$A_{jmn} = \langle z^j, \phi_m \phi_n \rangle \tag{95}$$

The trigonometric identities for products of trigonometric functions are used to convert the products to functions of the sums and differences of the respective arguments. The specific identities to be used are as follows.

$$\cos k_{zm} z \cos k_{zn} z = \frac{1}{2} \cos(k_{zm} - k_{zn}) z + \frac{1}{2} \cos(k_{zm} + k_{zn}) z \tag{96}$$

$$\sin k_{zm}z \cos k_{zn}z = \frac{1}{2}\sin(k_{zm} - k_{zn})z + \frac{1}{2}\sin(k_{zm} + k_{zn})z \quad (97)$$

$$\cos k_{zm}z \sin k_{zn}z = -\frac{1}{2}\sin(k_{zm} - k_{zn})z + \frac{1}{2}\sin(k_{zm} + k_{zn})z \quad (98)$$

$$\sin k_{zm}z \sin k_{zn}z = \frac{1}{2}\cos(k_{zm} - k_{zn})z - \frac{1}{2}\cos(k_{zm} + k_{zn})z \quad (99)$$

Utilizing these identities gives the following formulas for the elements A_{jmn}. If m and n are both even, then

$$A_{jmn} = \frac{1}{2}\langle z^j, \cos(k_{zm} - k_{zn})z\rangle + \frac{1}{2}\langle z^j, \cos(k_{zm} + k_{zn})z\rangle \quad (100)$$

If m is odd and n is even, then

$$A_{jmn} = \frac{1}{2}\langle z^j, \sin(k_{zm} - k_{zn})z\rangle + \frac{1}{2}\langle z^j, \sin(k_{zm} + k_{zn})z\rangle \quad (101)$$

If m is even and n is odd, then

$$A_{jmn} = -\frac{1}{2}\langle z^j, \sin(k_{zm} - k_{zn})z\rangle + \frac{1}{2}\langle z^j, \sin(k_{zm} + k_{zn})z\rangle \quad (102)$$

Finally, if m and n are both odd, then

$$A_{jmn} = \frac{1}{2}\langle z^j, \cos(k_{zm} - k_{zn})z\rangle - \frac{1}{2}\langle z^j, \cos(k_{zm} + k_{zn})z\rangle \quad (103)$$

5.2.2 Evaluation of arrays B_{jmn}

When integrals involving ψ occur, ik_r would be used in place of k_{zm} or k_{zn}. This permits the development of explicit formulas for the elements B_{jmn} which are very similar to the ones for the matrix elements A_{jmn}. If m and n are both even, then

$$B_{jmn} = \frac{\Re\langle z^j, \cos(k_{zn} + ik_r)z\rangle}{\cosh k_r} \quad (104)$$

If m is odd and n is even, then

$$B_{jmn} = \frac{\Im\langle z^j, \sin(k_{zn} + ik_r)z\rangle}{\sinh k_r} \quad (105)$$

If m is even and n is odd, then

$$B_{jmn} = \frac{\Re\langle z^j, \sin(k_{zn} + ik_r)z\rangle}{\cosh k_r} \tag{106}$$

Finally, if m and n are both odd, then

$$B_{jmn} = \frac{-\Im\langle z^j, \cos(k_{zn} + ik_r)z\rangle}{\sinh k_r} \tag{107}$$

Note that every even-numbered row of the array B_{jmn} is identical, as is every odd-numbered row. Thus, the complete array B_{jmn} is defined by $(2 \times N)$ elements.

5.2.3 Evaluation of arrays C_{jmn}

The formulas for the elements of the arrays C_{jmn} are found by letting both k_{zn} and k_{zm} go to ik_r. If m and n are both even, then

$$C_{jmn} = \frac{\langle z^j, 1\rangle + \langle z^j, \cos 2ik_r z\rangle}{1 + \cos 2ik_r} \tag{108}$$

If m is odd and n is even, then

$$C_{jmn} = \frac{\langle z^j, \sin 2ik_r z\rangle}{\sin 2ik_r} \tag{109}$$

If m is even and n is odd, then

$$C_{jmn} = \frac{\langle z^j, \sin 2ik_r z\rangle}{\sin 2ik_r} \tag{110}$$

Finally, if m and n are both odd, then

$$C_{jmn} = \frac{\langle z^j, 1\rangle - \langle z^j, \cos 2ik_r z\rangle}{1 - \cos 2ik_r} \tag{111}$$

Only a (2×2) array must be evaluated to provide all elements of C_{jmn}.

5.2.4 Evaluation of Elementary Integrals

Let the sums and differences of the vertical wavenumbers be designated as

$$\sigma_{mn} = k_{zm} \pm k_{zn} \tag{112}$$

All of the inner products in the previous section are evaluated using the following two elementary integrals.

$$\langle z^j, \sin \sigma_{mn} z \rangle \qquad \begin{cases} = 0, & \text{if } j \text{ is even} \\ \neq 0, & \text{if } j \text{ is odd} \end{cases} \tag{113}$$

$$\langle z^j, \cos \sigma_{mn} z \rangle \qquad \begin{cases} \neq 0, & \text{if } j \text{ is even} \\ = 0, & \text{if } j \text{ is odd} \end{cases} \tag{114}$$

The parameter σ_{mn} in equation 112 can be small or large. Diagonal elements in the array A_{jmn} have $\sigma_{mn} = 0$. The elements in the array C_{jmn} have terms where $\sigma_{mn} = 0$ or $|2ik_r|$, both of which are small if k_r is small, $|k_r| << 1$. Off-diagonal elements will generally have integrals where σ_{mn} is large. The integrals where $|\sigma_{mn}|$ is small or zero are best evaluated using power series for the sine and cosine functions. The following formulas presume that j is even or odd, depending on whether the integral has a non-zero value .

$$\langle z^j, \sin \sigma_{mn} z \rangle = \sum_{p=0}^{\infty} \frac{(-1)^p \sigma_{mn}^{2p+1}}{(2p+2j+2)(2p+1)!}, \quad |\sigma_{mn}| < O(1) \tag{115}$$

$$\langle z^j, \cos \sigma_{mn} z \rangle = \sum_{p=0}^{\infty} \frac{(-1)^p \sigma_{mn}^{2p}}{(2p+j+1)(2p)!}, \quad |\sigma_{mn}| < O(1) \tag{116}$$

When $|\sigma_{mn}|$ is a finite number, then exact expressions for the inner products are available.

$$\begin{aligned} \langle z^j, \sin \sigma_{mn} z \rangle &= -\frac{\cos \sigma_{mn}}{\sigma_{mn}} \sum_{p=0}^{[j/2]} \frac{(-1)^p j!}{(j-2p)! \sigma_{mn}^{2p}} \\ &+ j \frac{\sin \sigma_{mn}}{\sigma_{mn}^2} \sum_{p=0}^{[j/2]} \frac{(-1)^p (j-1)!}{(j-1-2p)! \sigma_{mn}^{2p}} \end{aligned} \tag{117}$$

$$\begin{aligned} \langle z^j, \cos \sigma_{mn} z \rangle &= \frac{\sin \sigma_{mn}}{\sigma_{mn}} \sum_{p=0}^{[j/2]} \frac{(-1)^p j!}{(j-2p)! \sigma_{mn}^{2p}} \\ &+ j \frac{\cos \sigma_{mn}}{\sigma_{mn}^2} \sum_{p=0}^{[j/2]-1} \frac{(-1)^p (j-1)!}{(j-1-2p)! \sigma_{mn}^{2p}} \end{aligned} \tag{118}$$

All of the finite-series expressions above are exact, and the condition on $|\sigma_{mn}|$ is a general recommendation for their application, but not an absolute requirement. The finite series are limited by machine accuracy, because their results are given as the differences of large numbers when $|\sigma_{mn}|$ is small. The two terms in the finite series are $O(|\sigma_{mn}|^{-2([j/2]+1)})$, and their difference must be $O(1)$. Consequently, any machine error ϵ_{min} is amplified by the magnitude of the two terms. If the desired computation error is less than ϵ, then $|\sigma_{mn}|$ is limited

$$\epsilon_{min}|\sigma_{mn}|^{-2([j/2]+1)} < \epsilon \tag{119}$$

The finite series should then be used if

$$|\sigma_{mn}| > (\frac{\epsilon_{min}}{\epsilon})^{\frac{1}{2[j/2]+2}} \tag{120}$$

If we attempt to make the computation error as small as the machine error, then $|\sigma_{mn}| > 1$ in the finite series. Achieving machine accuracy in the infinite series requires enough terms in the series such that the inverse of the factorial is less than ϵ_{min}, that is, p ranges from 0 to M, where M is the least integer satisfying the condition

$$\frac{1}{(2M+1)!} < \epsilon_{min} \tag{121}$$

For example, a 64-bit computer word corresponds to a machine error of about 10^{-15}, and $19! \approx 1.2x10^{17}$, so that $2M+1 = 19$, or $M = 9$ as an upper limit in the infinite series with $|\sigma_{mn}| \leq 1$ would be consistent with the goal of machine accuracy for a 64-bit word.

6 Application to Poiseuille Flow Stability

This section considers the application of the preceeding analysis to the stability of Poiseuille flow in a channel. This is the simplest case to consider because the matrix solutions can be made separately for the even modes and for the odd modes. The asymptotic behavior of the matrix elements for large indices gives approximate solutions for the higher modes. This approximate solution is given below, and then computational results will be shown for a test case.

Poiseuille flow is symmetric with $U(z) = 1 - z^2$. The velocity coefficients are then $\{u_j\} = \{1, 0, -1\}$. There is a single coefficient for the curvature of the velocity, $\{u_j''\} = \{-2\}$. The array A_{0mn} is δ_{mn}/α_n^2, the array B_{0mn} is identically zero, and the array C_{0mn} is $\delta_{mn}C_{0nn}$, so that the array D_{mn} is

$$\begin{aligned} D_{mn} &= \alpha_m\alpha_n\left(\frac{\delta_{mn}}{\alpha_n^2} - A_{2mn} - (-1)^{[m/2]}\cos\delta_m B_{2mn}\right) \\ &-2\ \frac{\alpha_m\alpha_n}{k_n^2}\left(\frac{\delta_{mn}}{\alpha_m\alpha_n} + (-1)^{[m/2]+[n/2]}\cos\delta_m\cos\delta_n C_{0mn}\right) \end{aligned} \quad (122)$$

The matrices for the Poiseuille flow may be formed using only even modes or only odd modes, since the flow profile is symmetric. This greatly simplifies the computations for Poiseuille flow. All indices are then either both even or both odd, and functions like β_n which depend only on the parity of the index can conveniently be designated by a parity index p.

$$p = \mod(\mathrm{m}, 2) = \mod(\mathrm{n}, 2) \quad (123)$$

6.1 Asymptotic approximations for finite k_r

Asymptotic approximations were developed previously for the vertical wavenumbers. Similar approximations are possible for the elements of the array D_{mn}. The approximations show the properties of the general eigenvalue problem and will lead to an asymptotic estimate of the eigenvalues of the Orr-Sommerfeld equation itself. The asymptotic formulas are developed following a reversed order from the evaluation formulas in the previous section, that is, the formulas for the elementary functions are developed first, then formulas for elementary integrals are given, and finally, the formulas for the arrays are enumerated.

6.1.1 Asymptotic formulas for wavenumber variables

All formulas to be given here assume that k_r is finite. We use less accurate formulas than the ones given previously for the vertical wavenumbers because the point of this development is to show general properties rather than to develop an accurate computational procedure.

The offset variable δ_n is given by a one-term approximation

$$\delta_n \sim \frac{\beta_p}{\kappa_n} + \cdots, \quad \kappa_n >> k_r \tag{124}$$

The vertical wavenumbers are given by two-term approximations.

$$k_{zn} \sim \kappa_n \left(1 - \frac{\beta_p}{\kappa_n^2} + \cdots\right), \quad \kappa_n >> k_r \tag{125}$$

The spherical wavenumbers k_n depend on the radial wavenumber and the vertical wavenumbers.

$$k_n \sim \kappa_n \left(1 - \frac{\beta_p - \frac{1}{2}k_r^2}{\kappa_n^2} + \cdots\right), \quad \kappa_n >> k_r \tag{126}$$

This result gives a simple formula for the characteristic frequencies of the cross-modes

$$\omega_n \sim -i\nu\kappa_n^2 \left(1 + \frac{k_r^2 - 2\beta_p}{\kappa_n^2} + \cdots\right), \quad \kappa_n >> k_r \tag{127}$$

The mode normalization constants are also easy to estimate with these results.

$$\alpha_n \sim \sqrt{2}\left(1 + \frac{\beta_p}{2\kappa_n^2}\right) + \cdots, \quad \kappa_n >> k_r \tag{128}$$

6.1.2 Elementary integrals

The elementary integrals with small arguments can occur only when the terms represent positions on the diagonals of the arrays and when $k_\pm$ is the difference of the wavenumbers. But in this case, the arguments are exactly zero. The elementary integrals are then

$$\langle z^2, \cos(k_{zm} - k_{zn})z\rangle = \frac{1}{3}, \quad m = n \tag{129}$$

In the more general case, the arguments are finite.

$$\langle z^2, \cos \sigma_{mn} z \rangle = \frac{\sin \sigma_{mn}}{\sigma_{mn}} \left(1 - \frac{2}{\sigma_{mn}^2} \right) + 2 \frac{\cos \sigma_{mn}}{\sigma_{mn}^2} \quad \sigma_{mn} \neq 0 \tag{130}$$

The array C_{0mn} is given by

$$C_{0mn} = \frac{1}{2} \left(1 + (-1)^p \frac{\sinh 2k_r}{2k_r} \right) \tag{131}$$

6.1.3 Asymptotic formulas for arrays

The asymptotic form for the array B_{2mn} shows that it is inversely proportional to κ_n^2.

$$B_{2mn} \sim \frac{2}{\kappa_n^2} (-1)^{[(n+2)/2)]} + \cdots \tag{132}$$

The general form of the array D_{mn} can be completed with as estimate of the array A_{2mn}. Two cases must be considered here. In the first case, the indices are equal, and the elements are of order unity. In the other case, the indices are unequal, and the elements are small. The case of equal scripts is given by

$$A_{2nn} \sim \frac{1}{6} + (-1)^n \frac{1 - 2\beta_p}{4\kappa_n^2} + \cdots \tag{133}$$

When the scripts are unequal, we use the exact equation 113 with the asymptotic form for the sum and difference of the offsets.

$$\delta_m \pm \delta_n \sim \left(\frac{1}{\kappa_m} \pm \frac{1}{\kappa_n} \right) \beta_p + \cdots \sim \pm \left(\frac{\kappa_m \pm \kappa_n}{\kappa_m \kappa_n} \right) \beta_p + \cdots \tag{134}$$

If m and n are nearly equal, that is, the elements are near the principal diagonal of the array, then this approximation is of order $(\kappa)^{-2}$ when the difference is taken and of order $(\kappa)^{-1}$ when the sum is taken. In either case, the next term is of order $(\kappa)^{-3}$, so that it consistent to use it in both cases with this understanding. This gives the following result for the difference of the wavenumbers.

$$k_{zm} \pm k_{zn} \sim (\kappa_m \pm \kappa_n) \left(1 \mp \frac{\beta_p}{\kappa_m \kappa_n} + \cdots \right) \tag{135}$$

These formulas give an asymptotic form for the inner product of z^2 and the cosine functions. First, express the exact integral in terms of the wavenumbers and offset variables.

$$\begin{aligned}\langle z^2, \cos(k_{zm} \pm k_{zn})z\rangle &= -(-1)^{\frac{m\pm n}{2}} \frac{\sin(\delta_m \pm \delta_n)}{(k_{zm} \pm k_{zn})} \\ &+ 2(-1)^{\frac{m\pm n}{2}} \frac{\cos(\delta_m \pm \delta_n)}{(k_{zm} \pm k_{zn})^2} \\ &+ 2(-1)^{\frac{m\pm n}{2}} \frac{\sin(\delta_m \pm \delta_n)}{(k_{zm} \pm k_{zn})^3}\end{aligned} \tag{136}$$

The sine and cosine of the offset variable pairs are given by

$$\sin(\delta_m \pm \delta_n) \sim \pm(\kappa_m \pm \kappa_n)\left(\frac{\beta_p}{\kappa_m\kappa_n}\right) + \cdots \tag{137}$$

$$\cos(\delta_m \pm \delta_n) \sim 1 - \frac{(\kappa_m \pm \kappa_n)^2}{2}\left(\frac{\beta_p}{\kappa_m\kappa_n}\right)^2 + \cdots \tag{138}$$

These formulas are used to give the terms in equation 136.

$$\frac{\sin(\delta_m \pm \delta_n)}{(k_{zm} \pm k_{zn})} \sim \pm\left(\frac{\beta_p}{\kappa_m\kappa_n}\right) + \cdots \tag{139}$$

$$\frac{\sin(\delta_m \pm \delta_n)}{(k_{zm} \pm k_{zn})^3} \sim \pm\frac{1}{(\kappa_m \pm \kappa_n)^2}\left(\frac{\beta_p}{\kappa_m\kappa_n}\right) + \cdots \tag{140}$$

$$\frac{\cos(\delta_m \pm \delta_n)}{(k_{zm} \pm k_{zn})^2} \sim \frac{1}{(\kappa_m \pm \kappa_n)^2}\left(1 \pm 2\frac{\beta_p}{\kappa_m\kappa_n}\right) + \cdots \tag{141}$$

The final asymptotic formula for the inner products of z^2 and the cosine functions is

$$\langle z^2, \cos(k_{zm}\pm k_{zn})z\rangle \sim (-1)^{\frac{m\pm n}{2}}\left[\frac{2}{(\kappa_m \pm \kappa_n)^2}\left(1 \pm 3\frac{\beta_p}{\kappa_m\kappa_n}\right) \mp \frac{\beta_p}{\kappa_m\kappa_n}\right] \tag{142}$$

This gives a simple result for the dominant term in the array A_{2mn}.

$$A_{2mn} \sim (-1)^{\frac{m-n}{2}} \frac{1}{(\kappa_m - \kappa_n)^2} + \cdots \tag{143}$$

6.1.4 Asymptotic formula for array D_{mn}

The above results produce an easy formula for the array D_{mn} which shows that the matrix is dominated by the diagonal elements. That is, the off-diagonal elements in any given row or column are smaller in magnitude than the diagonal element. The matrix is clearly dominated by the first line in equation 94 because the terms in the second line vary as κ_n^{-2}. In the first line, terms from the array B_{2mn} also vary as κ_n^{-2} so that they will be negligible in comparison to the dominant terms in A_{2mn}, which are of order one near the diagonal. Thus, a first-order estimate of the array D_{mn} for large row and column indices m, n is

$$D_{mn} \sim T_{mn} = \begin{cases} \frac{2}{3} & , \text{if } n = m; \\ (-1)^{\frac{m-n+2}{2}} \frac{2}{(\kappa_m - \kappa_n)^2} & , \text{if } n \neq m. \end{cases} \tag{144}$$

Since m and n have the same parity, they must differ by some multiple of 2. The elements of the diagonals adjacent to the principal diagonal then have magnitude $2/\pi^2$, or about $1/5$. The diagonal elements are all nearly $2/3$. This is the average value of the flow speed $U(z)$ for the present case of Poiseuille flow. The symbol T_{mn} is used because the matrix elements depend only on position with respect to the principle diagonal. Matrices of this type are called Toeplitz matrices. The matrix D_{mn} is asymptotic, when both row and column indices are large, to the Toeplitz matrix T_{mn}.

6.2 Geršgorin region and asymptotic eigenvalues

It is known from matrix theory [9] that the eigenvalues of a matrix must lie within a domain in the complex plane called the Geršgorin region. This region is the union of all points which lie within circular subdomains called Geršgorin disks. The center of each disk is a point given by a diagonal element of the matrix, and the radius of each disk is the sum of the absolute values of the off-diagonal elements in the corresponding row or column. This actually defines two Geršgorin regions, but, in the present case of a Toeplitz matrix, the row and column sums are identical so that the row-disks and column-disks are identical. The Toeplitz matrix here is particularly simple and the disk radii are bounded by an infinite series with known sum. This

bound is given by

$$R'_n = \frac{2|k_x|}{\pi^2} \sum_{\substack{d=-n \\ d\neq 0}}^{\infty} \frac{1}{d^2} < \frac{4|k_x|}{\pi^2} \sum_{d=1}^{\infty} \frac{1}{d^2} = \frac{2}{3}|k_x| \tag{145}$$

That is, each Geršgorin disk has the same radius, and this radius is less than the product of the average flow speed and the axial wavenumber. In the limiting case of cross-modes, the axial wavenumber approaches zero and the eigenvalue must approach the disk center, or the value of a diagonal element of the matrix.

The center of the Geršgorin disk is a good first guess for the eigenvalue even when the axial wavenumber is not zero, at least in the case of large mode index n where the disks are disjoint regions.

$$\omega_n \approx \tilde{\omega}_n = k_x D_{nn} - i\nu k_n^2 \sim \frac{2}{3}k_x - i\nu\kappa_n^2 \tag{146}$$

The real part of the approximate eigenvalue (disk center) is the product of the average flow speed and the axial wavenumber $k_x = k_r \cos\phi$, and the imaginary part of the wavenumber is identical to the complex frequency of the cross-stream mode.

Figure 9 depicts two Geršgorin disks as defined by the above equations. An eigenvalue, called ω_n must lie within the shaded domain centered at $\tilde{\omega}_n$. Since the disk radius is less than to the real part of the diagonal element, there is no possibility that the real part of the eigenvalue is negative when the axial wavenumber is positive. More generally, the sign of the real part of the eigenvalue must match the sign of the axial wavenumber k_x.

$$\Re[\omega_n] \text{ is } \begin{cases} > 0, & \text{if } k_x > 0; \\ < 0, & \text{if } k_x < 0. \end{cases} \tag{147}$$

The imaginary part of the eigenvalue may be positive or negative if the index n, is small, but, if

$$\nu\kappa_n^2 > \frac{2}{3}|k_x| \tag{148}$$

then the imaginary part of the eigenvalue would be required to be negative, and all eigenvalues meeting this criterion must then lie in the lower half of

the complex plane and represent stable modes. Modes with index n are then stable if

$$n > 2\left(\sqrt{\frac{2Re}{3\pi^2}} - 1\right) \tag{149}$$

The Geršgorin disks may intersect as shown in figure 9, but when the mode index is large, the disks become disjoint and each disk must contain a single eigenvalue. The condition for disjoint disks is

$$n > \left(\frac{4Re}{3\pi^2} - 3\right) \tag{150}$$

The Geršgorin criterion guarantees only that an eigenvalue lies within the

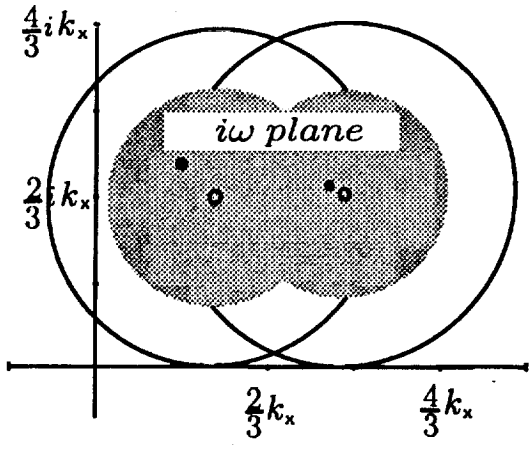

Figure 9: Geršgorin disks and eigenvalues for Poiseuille flow. The large circles are the outer bounds for the disks. Shaded areas are actual disks. Disk centers are open circular symbols and eigenvalues are filled circular symbols.

disk, not where it lies, but the computations in the following section will demonstrate that the eigenvalue approaches the disk center when the index is large. That is, the "higher" eigenvalues approach the centers of the Geršgorin disks.

6.3 Asymptotic convergence of eigenvalues

A simple approximation to the general eigenvalue problem for Poiseuille flow is given by the asymptotic eigenvalue problem.

$$\left[k_x \left[T_{mn}\right] - i\nu \left[\kappa_n^2\right]\right] \{ a_n \} = \omega \{ a_n \} \tag{151}$$

The matrices in this equation are within a few percent of the actual matrices so that this equation contains the principle features of the actual problem. This similarity is used here to demonstrate the convergence of the eigenvalues to the asymptotic formula. This is done by comparisons of results from the asymptotic formula and computations from 32nd order, 48th order, and 64th order matrices.

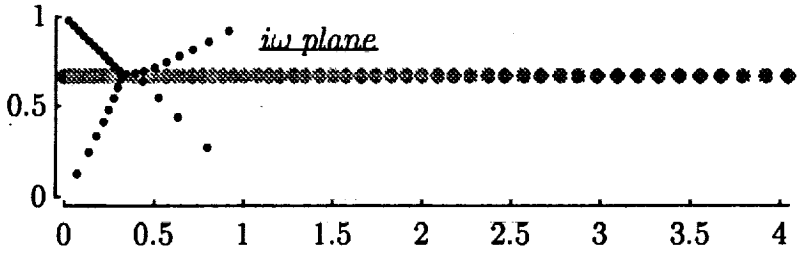

Figure 10: Even eigenvalues $i\omega$ for Poiseuille flow based on a 32nd order matrix, $k_r = 1$, $\phi = 0$, and Re $= 10^4$. Solid symbols represent computed eigenvalues using the Toeplitz matrix $[T]$ and the asymptotic values of the cross-mode wavenumbers, κ_n. Gray symbols represent the asymptotic formula for the eigenvalues.

Results from the 32nd order matrix solution are shown in figure 10. The 32 complex eigenvalues are distinct, and fall within a unit square in the 4th quadrant of the complex plane. This is a stable quadrant, according to the sign convention adopted for this paper. This approximate computation indicates flow stability, whereas it is known that this flow is theoretically unstable for Reynolds numbers above about 5772. But the purpose of these results is to show comparisons to the asymptotic formula, not make an absolutely accurate computation. The eigenvalues predicted by the asymptotic formula lie on a vertical line in the complex ω-plane which is defined by the average flow speed, 2/3. Since the length of this line gets large as more eigenvalues are added, the plot shows $i\omega$ to make the figure fit more comfortably on the

page. Note that only a few of the computed eigenvalues fall near the points generated by the asymptotic formlula. This is an indication that the selected matrix order is not sufficiently large.

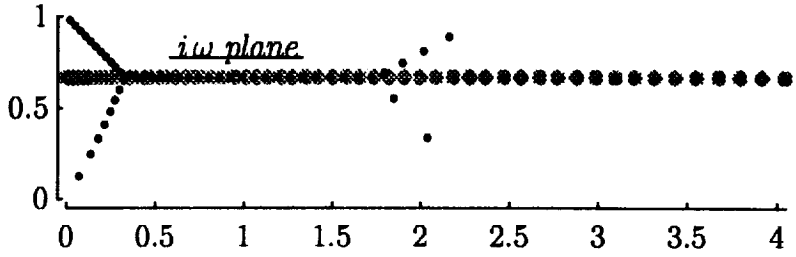

Figure 11: Even eigenvalues $i\omega$ for Poiseuille flow based on a 48th order matrix, $k_r = 1$, $\phi = 0$, and $\mathrm{Re} = 10^4$. Symbols are the same as in figure 10.

The results of computations using a 48th order matrix are shown in figure 11. It is seen that the more-attenuated eigenvalues have moved in the direction of the asymptotic formula results, while the less-attenuated eigenvalues are essentially unchanged. As expected, the increase in matrix size appears to produce a greater number of more-accurate eigenvalues. Eigenvalues from

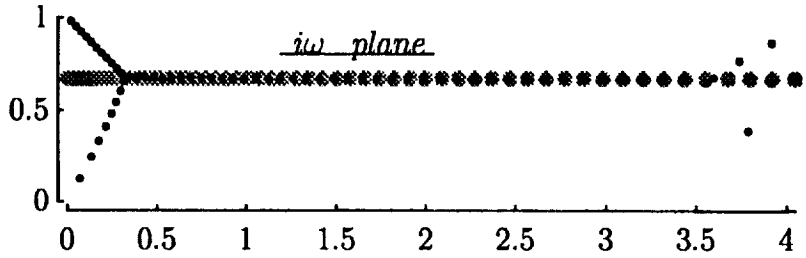

Figure 12: Even eigenvalues $i\omega$ for Poiseuille flow based on a 64th order matrix, $k_r = 1$, $\phi = 0$, and $\mathrm{Re} = 10^4$. Symbols are the same as in figure 10.

the 64th order matrix are shown in figure 12. It is seen that all but about 6 have approached the asymptotic results. It appears that the computed spectrum is approaching the asymptotic formula in the domain where the mode index n is large.

6.4 Computational results for Poiseuille flow.

The previous results show the qualities of the computation using an asymptotic approximation to the matrix eigenvalue problem. This section will show results of the actual matrix eigenvalue problem.

6.4.1 Numerical conditioning

The matrix eigenvalue problem with the cross-stream basis is well-conditioned in comparison to the Chebyshev/Tau method. This is demonstrated in figure 13 for the same physical case as in figure 3. That is, computations were made for the even modes using an order 32 matrix. As in figure 3, the computations were made with 32-bit and 64-bit words as a check of the sensitivity. Most of the 64-bit (black) eigenvalues plot directly onto the

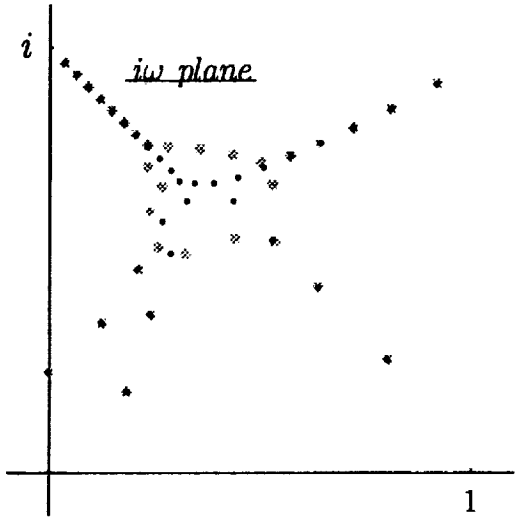

Figure 13: Even eigenvalues for Poiseuille flow using the Cross-Stream method and order 32 matrices. Symbols and physical parameters are the same as in figure 3.

the 32-bit eigenvalues, demonstrating the relative insensitivity to computer word size. More importantly, a careful count of the symbols shows that all 32 eigenvalues are accounted for within the displayed portion of the complex

plane. The eigenvalues are distinct, and a sorting operation on the imaginary part can then select a "least-attenuated" mode without the ambiguity of a partial eigenvalue list. There is, however, a discernable effect of word size on a few of the eigenvalues, so that the remainder of the computed results will be based on 64-bit words.

6.4.2 Asymptotic convergence of eigenvalues

Figure 14 shows the computations for a 64th order matrix. Again, gray symbols are the centers of the Geršgorin disks ($D_{nn} - i\nu k_n^2$) whereas the computed results are shown as black symbols. The radii of the Geršgorin disks will be roughly $(2/3)k_x$ so that the higher eigenvalues probably lie in the 4th quadrant. Inspection of figure 14 indicates that the computed eigenvalues lie even closer to the Geršgorin centers than in the case of the approximate matrix eigenvalue problem. Camparing figures 12 and 14 indicates that the Toeplitz matrix approximation affects primarily the lesser-attenuated modes which propagate at less than the average flow speed.

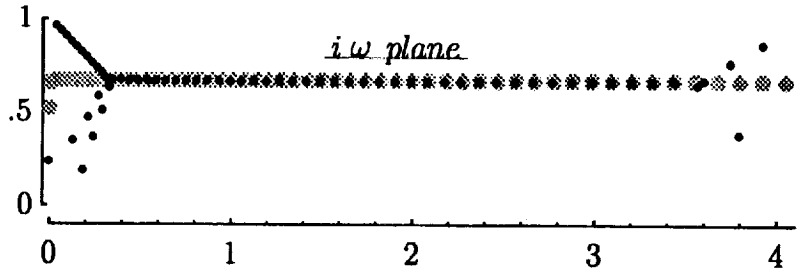

Figure 14: Even eigenvalues for Poiseuille flow using the cross-stream basis and order 64 matrices. Symbols and physical parameters are the same as in figure 12.

Figures 15, 16, and 17 show the convergence of the eigenvalues with increasing matrix size. The matrix order is doubled in each successive figure, starting from figure 15 where the order is 64, so that figure 16 has matrix order 128 and figure 17 has matrix order 256. figure 15 is the same 64-bit data as in figure 14, but only distance of the eigenvalue from the Geršgorin center is plotted. The abscissa in each figure is the actual mode index, which ranges up to 510 in figure 17. These computations show clearly that the eigenvalues converge to the Geršgorin centers as the index increases. It can be concluded

from this that the cross-stream method provides a means to compute an indefinite number of eigenvalues of the Orr-Sommerfeld equation. The first several hundred are computable by standard matrix eigenvalue algorithms, and any countable number of higher eigenvalues are approximated by the easily-computable Geršgorin centers.

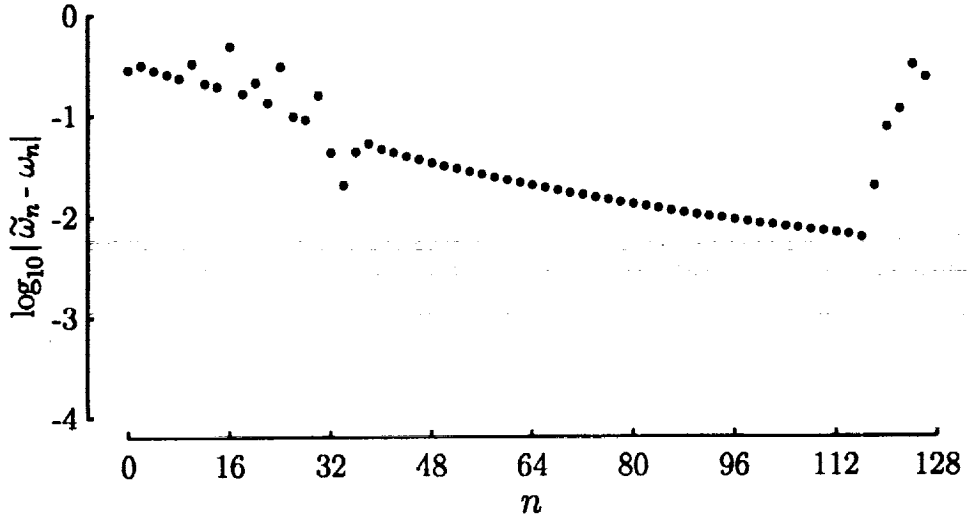

Figure 15: Distance of even eigenvalues from Geršgorin centers based on matrix order 64 computations. Physical parameters are the same as in figures 10–12.

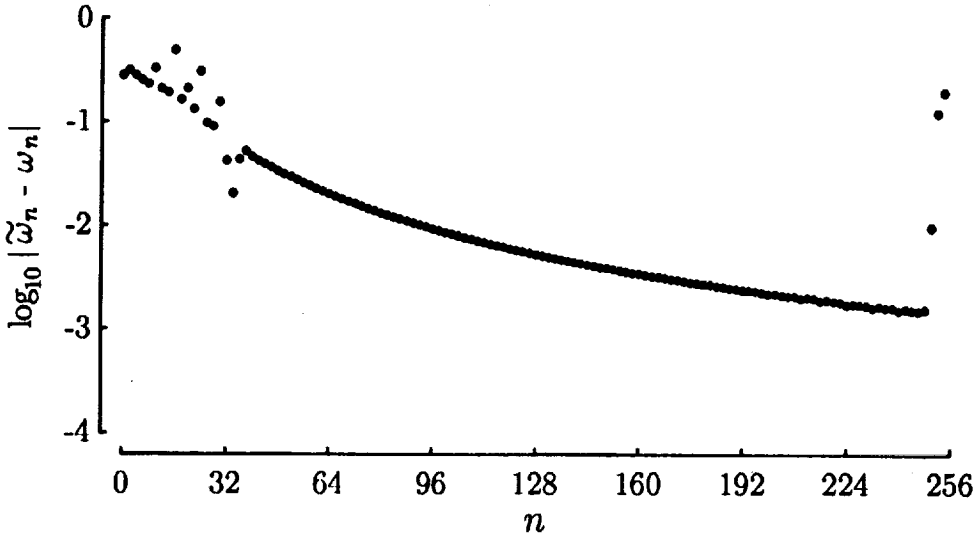

Figure 16: Distance of even eigenvalues from Geršgorin centers based on matrix order 128 computations. Symbols and physical parameters are the same as in figure 15.

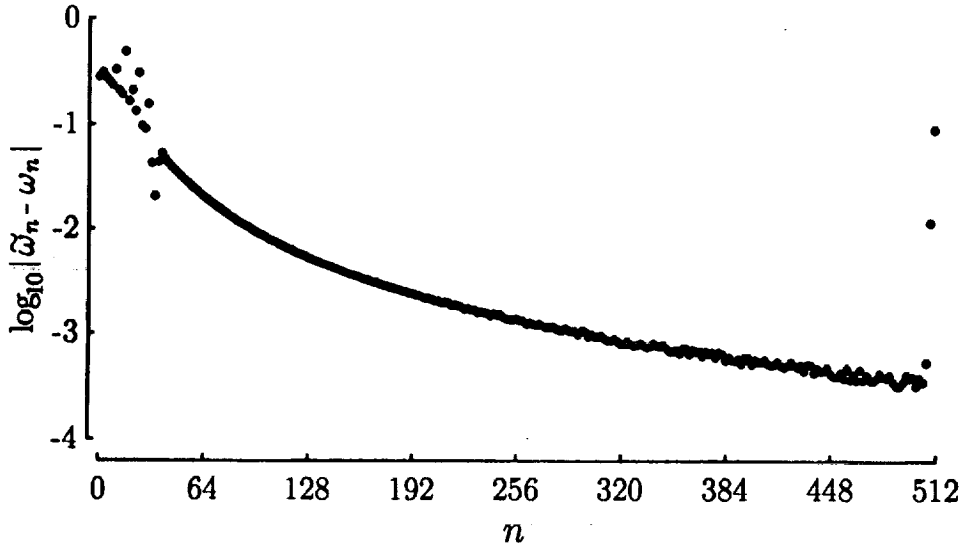

Figure 17: Distance of even eigenvalues from Geršgorin centers based on matrix order 256 computations. Symbols and physical parameters are the same as in figure 15.

7 Concluding Remarks

The Chebyshev polynomial basis for spectral solutions to the Orr-Sommerfeld equation leads to a generalized matrix eigenvalue problem. Matrices in this problem are ill-conditioned so that solutions require large computer words. The conditioning problem is exacerbated with increasing matrix order so that the Chebyshev basis can produce only a limited number of meaningful eigenvalues. The Chebyshev basis also produces eigenvalues in all four quadrants of the complex plane, even for cases believed to be stable, so that a definition of "least attenuated" mode is ambiguous.

Exact solutions to the Orr-Sommerfeld equation are available for waves propagating perpendicular to the flow direction. These solutions, called cross-stream modes here, are a countable set of linearly independent functions which serve as a basis for a Hilbert space. The cross-stream modes are not orthogonal, but may be subdivided into sets of even and odd functions which are, or course, orthogonal. The "angles" between each of the even functions are roughly 57°, and the angles between the odd functions are about 68°. The Hilbert space with this basis serves well to estimate the spectrum of the Orr-Sommerfeld operator and its boundary conditions.

The cross-stream basis leads to a standard matrix eigenvalue problem, which is simpler to solve than the generalized problem produced by the Chebyshev basis. Conditioning of this matrix eigenvalue problem is significantly better than the Chebyshev problem. The matrix is strictly diagonally dominant, and all matrix elements, for polynomial flow profiles, are given by known elementary integrals.

The matrix in the cross-stream eigenvalue problem approaches the sum of a constant real Toeplitz matrix and a complex diagonal matrix when the mode index is large. The complex diagonal represents the purely damped frequencies of the cross-stream modes, that is, the elements of this diagonal matrix are negative imaginary numbers.

The eigenvalues of the cross-stream matrix lie within well-defined Geršgorin disks. It has been shown that the radius of each disk, is less than about $2k_x/3$ for Poiseuille flow, where the fraction 2/3 represents the average speed of the flow and k_x is the given axial wavenumber. As the wavenumber decreases to zero, the disks become points and the eigenvalues are exactly the eigenvalues of the cross-stream modes. The Geršgorin disks for the cross-stream matrix show that the real part of all eigenvalues must have the same

algegraic sign as the given axial wavenumber. The Geršgorin disks show also that only a finite number of modes may be unstable, that is, have eigenvalues with a positive imaginary part. This number increases in proportion to the square root of the Reynolds number. An asymptotic formula has been developed for the "higher" eigenvalues, which are those with greater attenuation. The real part of the asymptotic eigenvalue is the product of the average flow speed and the axial wavenumber, and the imaginary parts are the negative-imaginary frequencies of the cross-stream modes.

Computations with the cross-stream method have been made for the well-studied case of a Poiseuille flow with Reynolds number 10,000. Matrix orders up to 256, producing 512 eigenvalues, half even and half odd, show that the lower eigenvalues match the results of the Chebyshev method to eight significant figures while the higher eigenvalues approach the asymptotic formula to within three significant figures.

Computations also show only a single eigenvalue with positive imaginary part. This is the one corresponding to the critical mode defined by other investigators. All other eigenvalues have negative imaginary parts. The cross-stream method permits an unambiguous definition of "least attenuated mode" through a sorting process on the imaginary part on all eigenvalues produced by the computation.

The cross-stream method is a well-conditioned and robust computational approach which can produce an essentially unlimited number of accurate eigenvalues of the Orr-Sommerfeld equation.

8 References

References

[1] S.Chandrasekhar. *Hydrodynamic and Hydromagnetic Stability.* Dover Publications, Inc., New York, 1981.

[2] P. G. Drazin and W. H. Reid. *Hydrodynamic Stability.* Cambridge University Press, New York, 1981.

[3] C. L. Dolph and D. C. Lewis. *On the application of infinite systems of ordinary differential equations to perturbations of plane Poiseuille flow.* Quarterly of Applied Mathematics, Vol. XVI, No. 2, pp 97–110, 1958.

[4] Chester E. Grosch and Harold Salwen. *The stability of steady and time-dependent plane Poiseuille flow.* J. Fluid Mech., Vol 34, part 1, pp. 177–205, 1968.

[5] Steven A. Orzag. *Accurate solution of the Orr-Sommerfeld stability equation.* J. Fluid Mech., Vol. 50, part 4, pp 689-703, 1971.

[6] T. J Bridges and P. M. Morris. *Differential Eigenvalue Problems in Which the Parameter Appears Nonlinearly* Journal of Computational Physics, Vol. 55, pp. 437–460, 1984.

[7] Francoise Chatelin. *Spectral Approximation of Linear Operators.* Academic Press, New York, 1983.

[8] *USER'S MANUAL, IMSL MATH/LIBRARY$^{T.M.}$. FORTRAN Subroutines for Mathematical Applications, Vol. 1, Chapter 2.* IMSL, Inc., 2500 ParkWest Tower One, 2500 CityWest Boulevard, Houston, Texas 77042-3020, USA, 1989.

[9] Roger A. Horn and Charles R. Johnson. *Matrix Analysis.* Cambridge University Press, New York, 1988.

[10] Gene H. Golub and Charles F. Van Loan. *Matrix Computations.* The Johns Hopkins University Press, Baltimore, 1989.

REPORT DOCUMENTATION PAGE

Form Approved
OMB No. 0704-0188

1. AGENCY USE ONLY *(Leave blank)*	2. REPORT DATE	3. REPORT TYPE AND DATES COVERED
	March 1993	Technical Memorandum

4. TITLE AND SUBTITLE

On the Cross-Stream Spectral Method for the Orr-Sommerfeld Equation

5. FUNDING NUMBERS

505-59-52

6. AUTHOR(S)

W. E. Zorumski and S. L. Hodge

7. PERFORMING ORGANIZATION NAME(S) AND ADDRESS(ES)

NASA Langley Research Center
Hampton, VA 23681-0001

8. PERFORMING ORGANIZATION REPORT NUMBER

9. SPONSORING/MONITORING AGENCY NAME(S) AND ADDRESS(ES)

National Aeronautics and Space Administration
Washington, DC 20546-0001

10. SPONSORING/MONITORING AGENCY REPORT NUMBER

NASA TM-107737

11. SUPPLEMENTARY NOTES

12a. DISTRIBUTION/AVAILABILITY STATEMENT

Unclassified-Unlimited
Subject Category 71

12b. DISTRIBUTION CODE

13. ABSTRACT *(Maximum 200 words)*

Cross-stream models are defined as solutions to the Orr-Sommerfeld equation which are propagating normal to the flow direction. These models are utilized as a basis for a Hilbert space to approximate the spectrum of the Orr-Sommerfeld equation with plane Poiseuille flow. The cross-stream basis leads to a standard eigenvalue problem for the frequencies of Poiseuille flow instability waves. The coefficient matrix in the eigenvalue problem is shown to be the sum of a real matrix and a negative-imaginary diagonal matrix which represents the frequencies of the cross-stream modes. The real coefficient matrix is shown to approach a Toeplitz matrix when the row and column indices are large. The Toeplitz matrix is diagonally dominant, and the diagonal elements vary inversely in magnitude with diagonal position. The Poiseuille flow eigenvalues are shown to lie within Gersgorin disks with radii bounded by the product of the average flow speed and the axial wavenumber. It is shown that the eigenvalues approach the Gersgorin disk centers when the mode index is large, so that the method may be used to compute spectra with an essentially unlimited number of elements. When the mode index is large, the real part of the eigenvalue is the product of the axial wavenumber and the average flow speed, and the imaginary part of the eigenvalue is identical to the corresponding cross-stream mode frequency. The cross-stream method is numerically well-conditioned in comparison to Chebyshev based methods, providing equivalent accuracy for small mode indices and superior accuracy for large indices.

14. SUBJECT TERMS

Spectral methods, Poiseuille flow, Flow stability, Orr-Sommerfeld Equation

15. NUMBER OF PAGES

46

16. PRICE CODE

A03

17. SECURITY CLASSIFICATION OF REPORT	18. SECURITY CLASSIFICATION OF THIS PAGE	19. SECURITY CLASSIFICATION OF ABSTRACT	20. LIMITATION OF ABSTRACT
Unclassified	Unclassified	Unclassified	